

Physical distinction between rolling-grain ripples and vortex ripples: An experimental study

Germain Rousseaux*

*Université de Nice–Sophia Antipolis, Institut Non-Linéaire de Nice, UMR 6618 CNRS-UNICE, 1361,
route des Lucioles, 06560 Valbonne, France*

(Received 25 July 2006; revised manuscript received 6 September 2006; published 7 December 2006)

We have performed an experimental study of the transition of rolling-grain ripples toward vortex ripples. In particular, we have looked for the influence of the grains' diameter, the frequency of oscillation, and the grains' cohesion. We demonstrate that the rolling-grain ripples are transient patterns which do appear as soon as we are close to the threshold for grain motion, whereas vortex ripples are always the final patterns observed and are the only patterns observed if one is far from the threshold for grain motion. Our results show that the "elasticity" (i.e., the tendency to modify the wavelength by either compression or dilatation) of the vortex ripples explains several discrepancies with respect to the observed evolutions and measurements reported so far in the literature.

DOI: [10.1103/PhysRevE.74.066305](https://doi.org/10.1103/PhysRevE.74.066305)

PACS number(s): 45.70.Qj

INTRODUCTION

When a fluid oscillates over sand grains, rippling patterns appear. The canonical examples are the ripple marks encountered close to the seashore. In order to reproduce such structures in the laboratory, Bagnold employed in 1946 an oscillating plate covered with a layer of sand in static water. He observed two types of "stable" pattern [1]: rolling-grain ripples (small patterns with grains moving back and forth at the interface between sand and water) and vortex ripples (larger patterns with a vortex detaching from the crest scooping grains from the neighboring sand structures). Since 1946, the two patterns have been treated independently until recently when it was observed that rolling-grain ripples become vortex ripples [2]. In this paper, we propose to assess Bagnold's distinction.

In this work, we examine the transition from a flat bed to a rippling pattern. In particular, we look for the range of parameters allowing us to observe rolling-grain ripples for a long time and their transition to the vortex ripple regime. We modify mainly the diameter of the glass beads, their cohesion, and the oscillation frequency.

EVOLUTION OF A FLUID-GRANULAR INTERFACE UNDER AN OSCILLATING FLOW

We use two similar setups which differ by their size. The experimental setups, measurements, and procedures were already described in [3] for the old setup and in [4] for the new one (Fig. 1). Essentially, it consists in an alternative arrangement of Bagnold's experiment but which does not induce different results: a layer of sand (spherical glass beads in practice) resting on a plate and immersed in a static water of kinematic viscosity ν is put into oscillation at a definite amplitude A (a few centimeters) and frequency f (around 1 Hz). The grains of diameter d (between 65 and 325 μm) are sheared by the fluid. More precisely, a viscous boundary layer $\delta = \sqrt{\nu/(\pi f)}$ develops at the interface between the sand

and the water. If $d \ll \delta$, the fluid flow is similar to the one obtained in the case when the bed is static and the fluid is in motion (see the additional note by Taylor in an Appendix of Bagnold's paper [1]). Then, subsequent grain movements induce the appearance of a periodic deformation of the granular-fluid interface that we identify with ripples. We design a cylindrical geometry in order to have periodic boundary conditions. Indeed, the layer of sand fills the gap between two concentric cylinders attached to a circular plate. Water is then added and we close the entire setup with a top plate (that is, the two cylinders) which is made to oscillate in a sinusoidal way by a brushless motor. Above the bed (4 cm in height), the water (5 cm in height) is at rest except in the three boundary layers: one at the interface and two on the vertical walls of both cylinders. With respect to the last ones, the gap (1.9 cm) between the cylinders is much more important than the size of the boundary layers at the usual frequencies used in this work (for example, $\delta = 564 \mu\text{m}$ at $f = 1 \text{ Hz}$).

The shape of the ripples

First, let us illustrate by some pictures the definitions given by Bagnold in his seminal papers with respect to the shape and evolution of both types of ripples [1]. A charge-coupled device (CCD) camera attached by a metallic arm on the side of the new setup allows us to have access to the forms (Fig. 2) and the dynamics of the ripples in the moving frame of reference (Fig. 3: white and black correspond to the crests and the troughs of the patterns; hence, the gray levels stand for different ripple heights). As described by Bagnold, rolling-grain ripples are small bumps of triangular shape with a rounded crest separated by an almost horizontal interface whereas vortex ripples are more pronounced triangular patterns without a flat separation between them (Fig. 2). The spatiotemporal diagram gives us some clues to the duration of each ripple regimes (Fig. 3). Indeed, for the particular parameters used in the experiments, rolling-grain ripples are characterized by a lot of coalescence events compared to vortex ripples which do reach a stationary state more rapidly. We can also infer the velocity of propagation of the front of vortex ripples (let us recall that Bagnold used the expression

*Electronic address: Germain.Rousseaux@inln.cnrs.fr

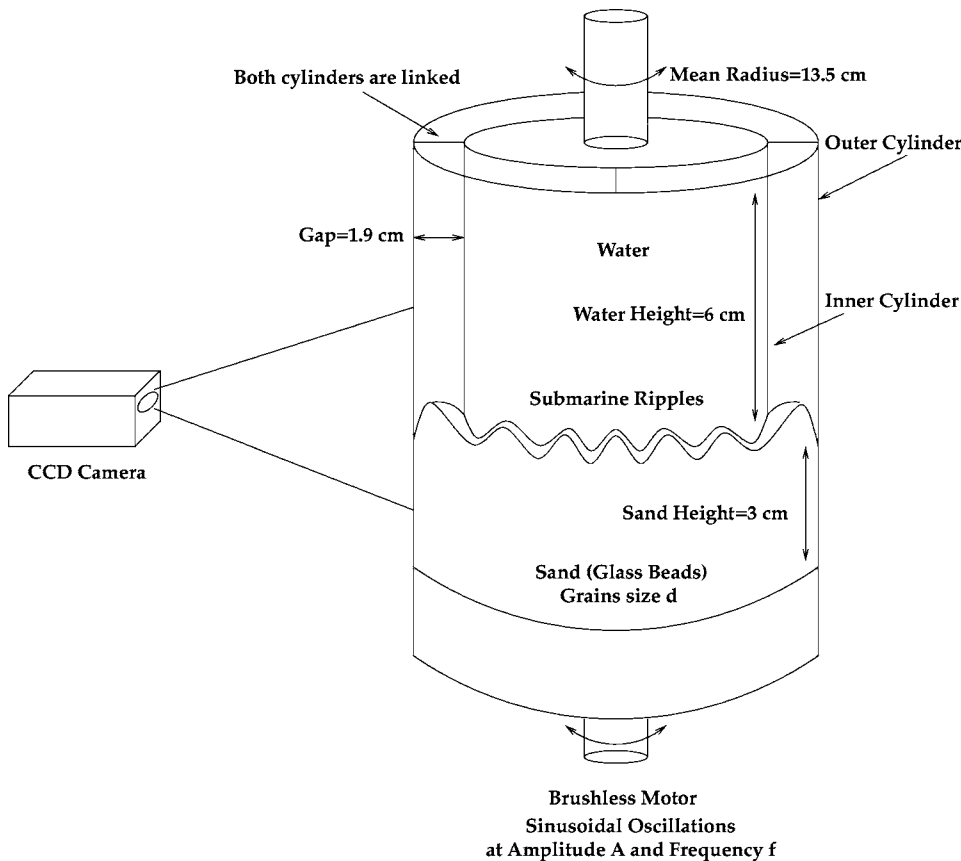


FIG. 1. Scheme of the new experimental setup. The vertical scale is dilated.

“like a disease” to denote the front propagation [1]). Moreover, a large-scale deformation of the interface is visible in particular in the final state of vortex ripples as the mean gray level varies with a wavelength equal to the perimeter.

Undulations of the crests

As reported by Bagnold [1], rolling-grain ripples are granular structures which are characterized by a strong variation of the crest’s shape every half period whereas the space between two neighboring ripples is less active. The crest is oscillating with the flow and one cannot say that rolling-grain ripples are truly symmetric patterns because, if we stop the flow oscillations, the orientation of the crest is dictated by that of the fluid before the stop. On Fig. 4, we provide a clear picture of this process (as previously, the camera is oscillating with the plate and we look on the side of the outer cylinder): one distinguishes (on the spatiotemporal scale of a horizontal line placed just above the flat part of the interface: dark is in water and white represents sand bed protuberances which cross the line of reference) the oscillations corresponding to each half period of several crests as well as a coalescence between two ripples (see below for details). The cylinder curvature does not affect our results since the size of the camera frame (2.7 cm) is much smaller than the mean radius (13.5 cm). The same effect exists for the vortex ripples but is less important as the protuberance is likely to be destroyed by its resuspension due to the flow at each half period.

THE PHENOMENOLOGY ASSOCIATED WITH THE COALESCENCE OF RIPPLES

Figure 5 displays the coalescence by fusion of two rolling-grain ripples. We have underlined the existence of undulations of the crests. This undulation is symmetric if the flow intensity is identical in both direction. When two ripples are close together, the flow velocity slows down in the trough between them which becomes, using the expression introduced by Andersen [5], a “shadow” zone for the oscillating flow (the flow is weaker behind the ripple, which is similar to a backward facing step). The crests of both ripples are likely to orient themselves toward the trough as the shear stress created by the background flow is no longer symmetric (Fig. 4). The grains accumulate subsequently and fill the space between two ripples until their coalescence. Hence, an increase of the mean wavelength is always associated with a decrease of a local wavelength.

This type of coalescence is similar to the so-called translation mode within the thin-film community [6]. Despite the fact that numerous examples of coalescence exist in nature, the particular example of dewetting is particularly well documented in the literature concerning the mode of fusion. Indeed, dewetting of a thin film on a homogeneous substrate leads to fluid patterns with a typical length scale. The new drops have a radius which then increases monotonically in time through a coarsening process. One usually describes such an evolution with a Cahn-Hilliard type of equation. Moreover, as described in our previous work on the coalescence of rolling-grain ripples, the coarsening of this type of

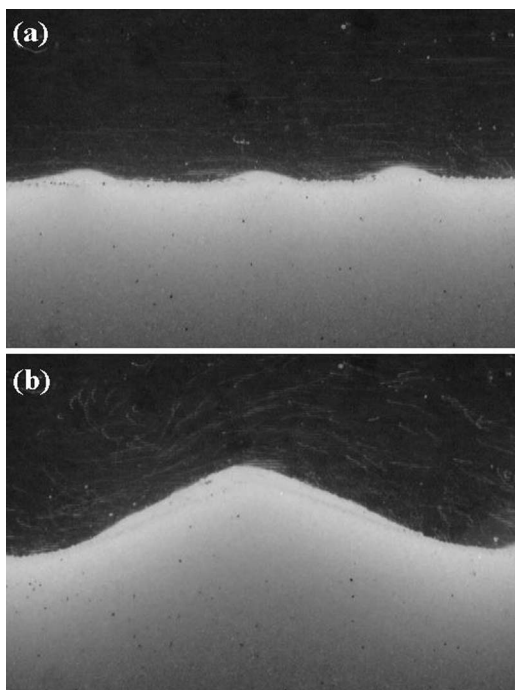


FIG. 2. The shape of ripples in the new setup (real scales): (a) rolling-grain ripples; (b) vortex ripples. The parameters are $f = 1$ Hz, $A = 1.5$ cm, and $d = 110 \mu\text{m}$. The width of the images is 2.7 cm.

ripple seems to follow a logarithmic behavior as a function of time for the mean wavelength as well as for the root mean square of the height (without the large-scale deformation) and this is typical of a Cahn-Hilliard coalescence in one dimension [3]. The thin-film community distinguishes the translation mode for coalescence from the mass-transfer mode. This other mode is characterized by transfers of mass from a single pattern to its left and right neighbors contrary to the translation mode which is mainly characterized by a fusion of two neighboring patterns [6]. The mass-transfer mode is a typical signature of the vortex ripples. We have already illustrated this mode in our work on the influence of segregation by showing the existence of the so-called cat's eyes patterns which demonstrate that vortex ripples swallow their neighbors [7]. This distinction between the two modes is very important since this is a sharp criterion in order to separate the rolling-grain ripples from the vortex ripples. As a matter of fact, we have shown in another previous work that the old criterion introduced by Bagnold, that is, the ab-

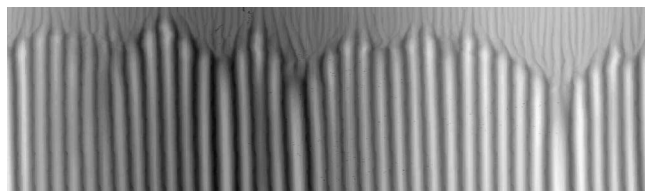


FIG. 3. Spatiotemporal diagram of the interface seen from the interior of the inner cylinder in the new setup with a conical mirror. Time is flowing downward. Same parameters as Fig. 2 and a final time of roughly one day.

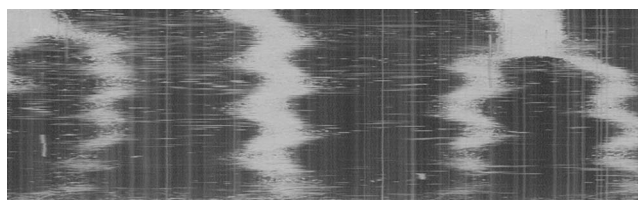


FIG. 4. Spatiotemporal diagram in the new setup (with the embarked camera on a side of the outer cylinder) along a horizontal line parallel to the initial flat interface and just above it. Time is flowing upward. Same parameters as Fig. 2 and a duration of about 5 s. The crests of the patterns are inclined in the opposite direction twice per period.

sence of a vortex over rolling-grain ripples is questionable as a viscous eddy is present over the rolling-grain ripples at each flow reversal [4]. Hence, in some sense, rolling-grain ripples are vortex ripples.

THE VORTEX RIPPLES

Whatever is the initial state of the interface (flat, with indentations, deformed at a large scale), the final state of a fluid-granular interface under an oscillating flow (with grain motion and without fluidization) is a vortex ripple state.

The elasticity of vortex ripples

We have encountered a major difficulty in determining the final wavelength of the vortex ripples. A review of the correlations proposed in the literature can be found in [8]: the final wavelength is proportional to the amplitude of oscillation A and is independent of both the grain's diameter d and the frequency f . The diameter changes only the forcing necessary to put the grains into motion. To simplify, if the grain size increases, one must increase the forcing (either A or f) [3]. The frequency independence was noticed first by Bag-

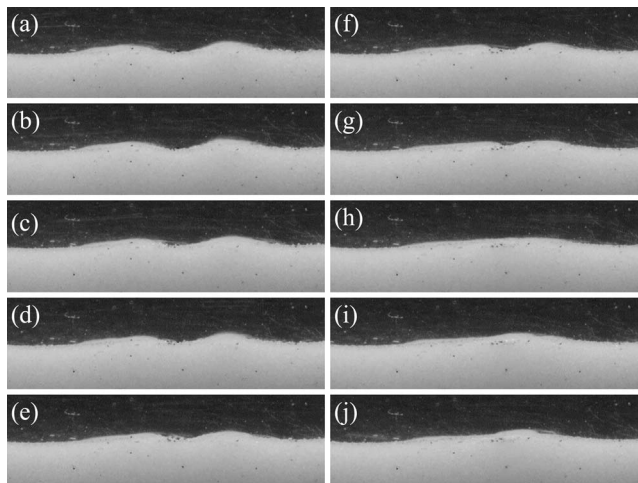


FIG. 5. A series of images describing the coalescence by a translation mode of two rolling-grain ripples (the time interval is 20 s between each picture for the parameters $f = 1$ Hz, $A = 1.5$ cm, and $d = 110 \mu\text{m}$). New setup.

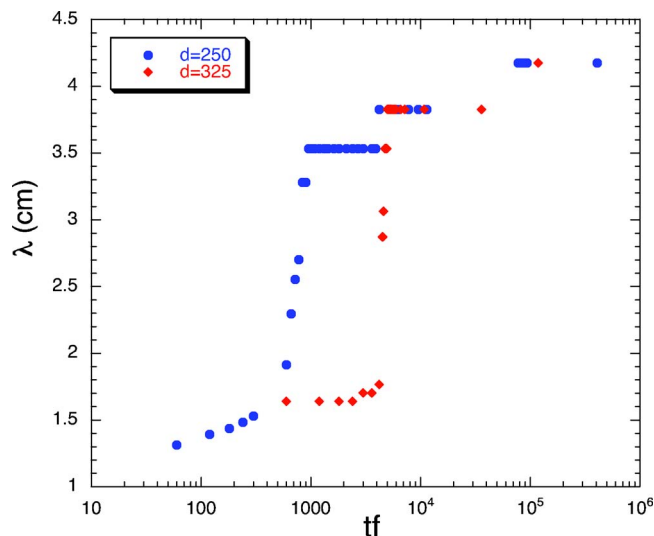


FIG. 6. (Color online) Ripple wavelength for two grain sizes (250 and 325 μm) as a function of time (linear-log scale). Old setup. Parameters are $f=1$ Hz, $A=2.45$ cm.

nold. We have shown that the frequency changes both the height and the shape of the final vortex ripples in our previous work on segregation [7].

In this work, where the parameters were varied in a large extent, we noticed several deviations from the so-called 4/3 law [2] and we attribute these discrepancies to the elasticity of the system of vortex ripples, a term introduced by Bagnold in his 1946 paper. Let us illustrate this point [1]. In Fig. 6, we display two typical evolutions of the mean wavelength of the ripples (see in addition [3]). For the following discussion, we will focus on the evolution associated with the grain size $d=250$ μm . If one had stopped the measurements at 4000 oscillations because the ripple wavelength was not evolving any more since 1000 oscillations, one would have made an error of 20% on the final wavelength measured at 100 000 oscillations. The difficulty is that the experimenter has the (wrong) impression that the system of ripples is stabilized. We notice that the wavelength jumps by quanta as a single ripple “disappears” at each coalescence.

It seems that this evolution through several plateaus is the illustration of the elasticity described by Bagnold. Indeed, at the moment of the transition from the rolling-grain ripples to the vortex ripples, several rolling-grain ripples become at the same time vortex ripples. Hence, the number of nucleation spots is important and so is the number of systems of vortex ripples which will compete in order to invade the whole setup extent. Each system tries to occupy the largest place and is in competition with the other systems. We have observed that the whole system blocks itself in a kind of metastable state for which it had not reached the final wavelength, as it would have done if it had started from a single site of nucleation. The mean wavelength does not change but the profile of the ripples can vary. Sometimes, we even observe an accordion shape of the envelope of the ripples’ height. This behavior is similar to the so-called Eckhaus instability of one-dimensional patterns by successive compressions and dilatations of the system of ripples until one or several ripples is (are) annihilated [9].

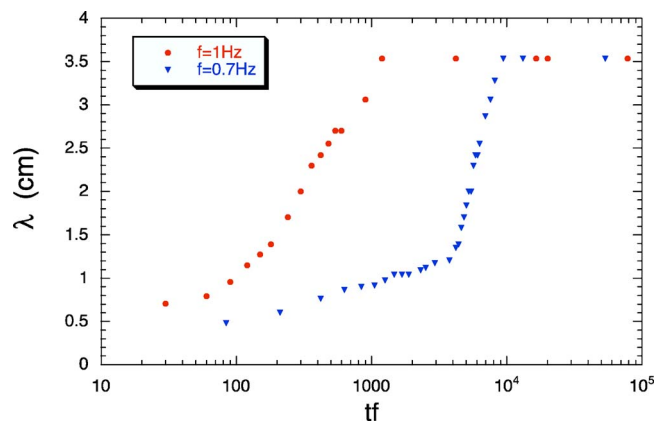


FIG. 7. (Color online) Ripple wavelength for two frequencies (0.7 and 1 Hz) as a function of time (linear-log scales). Old setup. Parameters are $A=2.45$ cm, $d=110$ μm .

Contrary to Bagnold who used a deep mark in the sand as a unique site of nucleation for a system of vortex ripples [1], our present experiments often feature these plateaus in the evolution as we started from a flat bed in order to study the evolution of the rolling-grain ripples. Hence, the error due to the elasticity can explain some discrepancies in the literature about the large number of correlations for the final wavelength of the vortex ripples. So, it is necessary to specify the initial state of the interface (flat or not) [10]. In addition, our setup has periodic boundary conditions because we use a cylindrical geometry and this can also explain such an evolution by recalling that other boundary conditions exist depending on the geometry [10–15].

The influence of the frequency of oscillation on the final wavelength of vortex ripples

Bagnold seems to have been the first to point out the independence of the final wavelength of the vortex ripples with the oscillation frequency [1]. We display such a behavior on Fig. 7 for two different frequencies. In addition, we provide an experimental demonstration that the evolution and more precisely the shape of the curve depend on the frequency. We will come back to the influence of frequency during the coarsening of the rolling-grain ripples.

Moreover, as noticed already by Bagnold, we do observe an increase of the wavelength that is the formation of typically one additional ripple when the frequency is such that one is close to the threshold value for fluidization. In our previous study dealing with the influence of segregation in a binary mixture, we have already noticed the presence of an additional ripple as can be seen in Fig. 6(f) of our paper [7]. This new ripple can disappear and appear again as the final state is a dynamical one. That is why Bagnold described it as an “oil bump” undulating horizontally [1].

THE PSEUDOSTABILITY ZONE OF ROLLING-GRAIN RIPPLES

Scherer *et al.* [16] as well as Stegner and Wesfreid [2] have shown that rolling-grain ripples are transient patterns

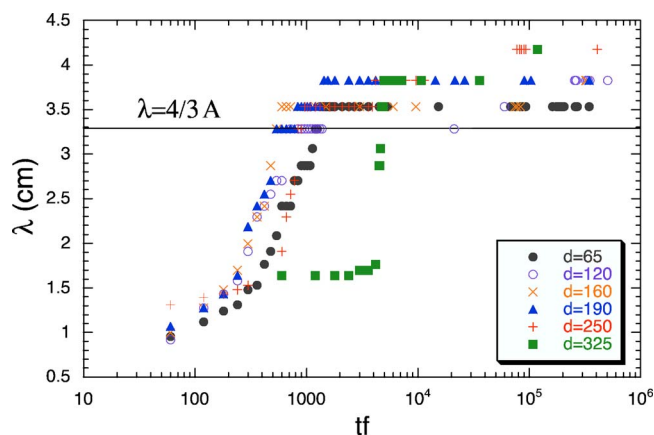


FIG. 8. (Color online) Ripple wavelength for several grain sizes (65,120,160,190,250, and 325 μm) as a function of time (linear-log scales). Old setup. Parameters are $f=1$ Hz, $A=2.45$ cm.

which do evolve always toward a stable vortex ripple state. However, several authors like Bagnold [1], Sleath [17], and Blondeaux [18] have reported the observation of stable rolling-grain ripples. Chan *et al.* even observed only rolling-grain ripples and not vortex ripples for very viscous liquids [19]. In our previous work [3], we have shown that rolling-grain ripples could evolve on a very long time scale if, for fixed frequency and grain diameter, one diminishes the amplitude of oscillation in order to get close to the threshold for motion. Hence, in this study we will confirm such a behavior if, for fixed amplitude and grain diameter, we decrease the frequency or if, for fixed amplitude and frequency, we increase the grain diameter. The major result is that the duration of the coarsening in the rolling-grain ripples state is longer if one is near the threshold for motion as discussed in our former paper on the subject [3] by evaluating the so-called Shields number (see below for a definition). We have called the coarsening phase “the pseudostability zone” of rolling-grain ripples despite the fact that they always evolve toward vortex ripples.

The influence of the grain size on the pseudostability zone

In order to bound the pseudostability zone of rolling-grain ripples, we first fix the amplitude of oscillation ($A=2.45$ cm) and the frequency ($f=1$ Hz) for several grain sizes $d=65,120,160,190,250$, and $325 \mu\text{m}$. The case of $65 \mu\text{m}$ needs a special discussion. On Fig. 8, the behavior of the ripples’ wavelength is very similar for the sizes $d=120, 160$, and $190 \mu\text{m}$ between 60 and 600 oscillations. The initial wavelengths are close together with a tendency toward an increase with the grain size. The transition toward vortex ripples happens around 250 oscillations for these three sizes. Above 600 oscillations, we notice that, the smaller the size is, the longer the wavelength stays on successive plateaus for a certain time. For example, the wavelength goes from 3.3 to 3.5 and then to 3.8 cm: for $d=120 \mu\text{m}$, the jump toward the first plateau happens around 20 000 oscillations, whereas it happens around 800 oscillations for $d=190 \mu\text{m}$, and so on. We follow this tendency for the two bigger sizes $d=250$ and

$325 \mu\text{m}$: the more the size increases, the less time the system spends in the intermediate plateaus. As an example, for $d=325 \mu\text{m}$, the system goes directly to the plateau with wavelength equal to 3.8 cm. In addition, the initial wavelength increases a lot for these big sizes and it is all the more difficult to observe the initial structures as we are able to detect them only after a while. This critical slowing down is reminiscent of the thermodynamic transitions in statistical physics.

However, we notice that the increase of size lengthens the typical time of transition t_T toward the vortex ripples state: $t_T f=500$ oscillations for $d=250 \mu\text{m}$ and $t_T f=4500$ oscillations for $d=325 \mu\text{m}$. Hence, the bigger the grain size, the longer the pseudostability zone, and the less the vortex ripples go through several intermediate plateaus. As discussed in our previous work, it is easy to understand that the increase of grain size pushes the system close to the threshold for motion described by the so-called Shields number which is defined by the ratio between the shear stress impressed by the fluid and the reduced weight of the grains ($\Theta \approx 1/d$) [3,19]. For the smaller grain sizes $d=120, 160$, and $190 \mu\text{m}$, the grain transport by the flow is so strong that the system evolves very rapidly toward the vortex ripple state as we are not able to distinguish any difference in the corresponding evolutions.

As discussed previously, the plateaus are the outcome of the ripple elasticity, that is, of the difficulty in annihilating additional ripples because of the competition between several ripple systems issuing from different nucleation sites.

Bagnold reported also that the presence of a unique nucleation site avoids the blocking of the wavelength evolution. Indeed, the smaller the grains, the shorter the initial wavelength, and hence the bigger the number of initial ripples is. By evolving, these ripples become nucleation sites for vortex ripples. As a consequence, if we increase the grain size, the number of ripples decreases and so does the number of nuclei, that is, the probability to block the ripple system in an intermediate plateau. Moreover, for the big sizes, the grain transport slows down as one approaches the motion threshold. However, if one rolling-grain ripple becomes a vortex ripple before the others, the transport associated with the newly formed vortex ripple will be larger. Hence, the system of vortex ripples created by this initial nucleus will invade faster the remaining rolling-grain ripples which do evolve on a longer time scale toward the vortex ripple state at the same time. So the probability of appearance of new systems of vortex ripples which would enter into competition with the first one diminishes.

Now, these conclusions seem doubtful if one considers the smaller size ($d=65 \mu\text{m}$). Indeed, despite the fact that the corresponding initial wavelength is small and of the same order for $d=120 \mu\text{m}$, the transition toward the vortex ripples happens at a time similar to the one associated with the size $d=250 \mu\text{m}$. We think that this behavior is the consequence of the cohesive character of the grains which appears for sizes smaller than $100 \mu\text{m}$ for glass beads. For this type of grain, the Shields number ($\Theta \approx 1/d$) does not take into account the interparticular cohesion and is no longer a good control parameter [3,20]. Hence, cohesive grains behave as bigger grains. If so, one gets closer to the threshold for mo-

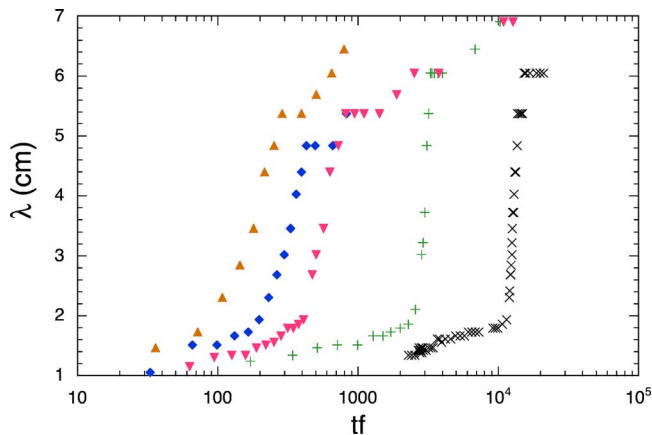


FIG. 9. (Color online) Ripple wavelength for several frequencies (0.425, 0.475, 0.525, 0.55, and 0.6 Hz) as a function of time for noncohesive grains (linear-log scale). Old setup. Parameters are $A = 5.75$ cm, $d = 200$ μm .

tion. That is why grains with size 120 μm are smaller in some sense than those with $d = 65$ μm because of the cohesion effect.

Finally, we found, as did Bagnold, that the interface between two crests is flat for sizes up to $d = 190$ μm ; then it becomes an arc of a circle for bigger sizes.

The influence of oscillation frequency on the pseudostability zone

As usual now, we notice the presence of several intermediate plateaus during the vortex ripple regime on Fig. 9 ($d = 200$ μm). Hence, as discussed previously, the measured “final” wavelength of vortex ripples depends in fact on the patience of the experimenter. But here we are not interested in the final wavelength but in the evolution from rolling-grain ripples toward vortex ripples. In addition, we have shown previously the independence of the final wavelength on the frequency if one waits sufficiently.

Now, if we decrease the frequency, the coalescence of rolling-grain ripples is longer as one gets close to the threshold for motion (crosses at 45° on Fig. 9). The duration of the coarsening lasts from a few seconds to several days depending on the frequency. This last fact explains how several workers on the subject were misled and thought that rolling-grain ripples could be stable patterns.

For the higher frequency (upward triangles on Fig. 9), one switches very rapidly from a flat bed to a vortex ripple regime and the rolling-grain ripples are almost unobservable. We can understand now why some other workers claimed that they did not observe rolling-grain ripples.

The major result here is that the wavelength of transition between rolling-grain ripples and vortex ripples is independent of the frequency, contrary to our previous study where we show that it does increase with the amplitude of oscillations [3] and the grain size (present study).

The behavior of the root mean square value of the ripple height around the interface is similar to the one of the wavelength (we suppressed the mean height of the interface,

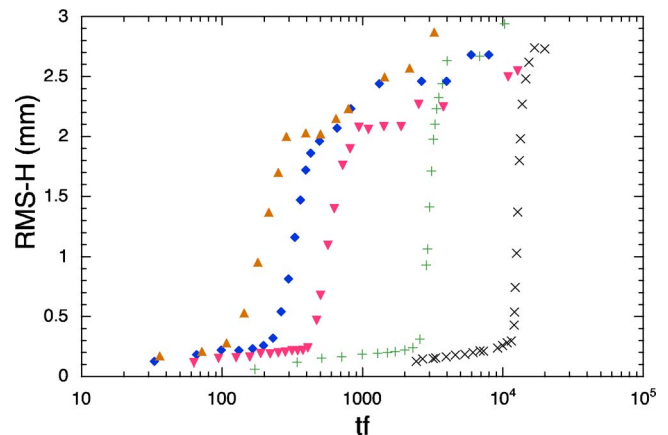


FIG. 10. (Color online) Root mean square value of the ripple height for several frequencies (0.425, 0.475, 0.525, 0.55, and 0.6 Hz) as a function of time for noncohesive grains (linear-log scale). Old setup. Parameters are $A = 5.75$ cm, $d = 200$ μm .

which can vary because of different initial conditions [3]). We notice that the transition from rolling-grain ripples to vortex ripples happens for a fixed value around 0.25 mm whatever is the frequency (Fig. 10). The same value is valid for any grain size and amplitude (we do not report the plots here) so can be considered as a universal value for the transition of an interface.

Finally, we did observe (with a fast CCD camera), as did Bagnold, the fact that the path of the grains increases with the frequency (and the amplitude [3]). It seems that rolling is really a feature of rolling-grain ripples. Indeed, when the frequency is high rolling is replaced by lifting and one goes directly from a flat bed to the vortex ripple state, bypassing the rolling-grain ripple state. Contrary to what was asserted by Bagnold, we do observe motion within the ripple troughs by image subtraction, but it is less active than above the crests.

The influence of grain cohesion on the pseudostability zone

We have seen that the time scale for the transition was modified by interparticular cohesion. This cohesion is of physical and not chemical origin and certainly due to van der Waals forces between the glass beads immersed in distilled water. However, a detailed study should be done on this latter point.

We decided to check if the global behavior for the smaller size ($d = 65$ μm) was different from the others. We did not find any discrepancies in the evolution for either the wavelength (Fig. 11) and the root mean square value of the ripple height (Fig. 12).

As a partial conclusion, cohesion does not affect the global ripple evolution but modifies the time scale by slowing down the coalescence. Future studies should concentrate on the influence of additional phenomena like chemical cohesion encountered at the beach due to the seawater properties.

CONCLUSIONS AND PERSPECTIVES

We hope that our study has clarified the physical distinction between rolling-grain ripples and vortex ripples. We

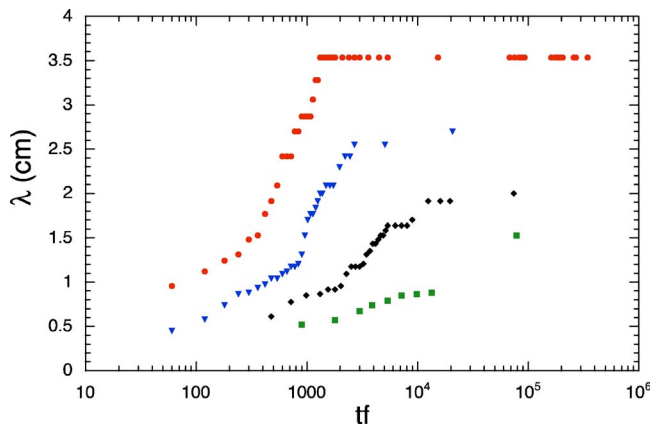


FIG. 11. (Color online) Ripple wavelength for several amplitudes (0.91, 1.22, 1.84, and 2.45 cm) as a function of time for cohesive grains (linear-log scale). Old setup. Parameters are $f=1$ Hz, $d=65$ μm .

have looked for the influence of the frequency of oscillation, the grain diameter, and the interparticle cohesion. We have confirmed our previous findings concerning the fact that the rolling-grain ripples can be observed provided that the threshold of grain motion is within the range of parameters used in the experiment. Otherwise, if one is far from it, only vortex ripples are present. Additional works are nonetheless needed to sharpen the picture presented here. In particular, to what extent is the mode of grain transport (rolling or lifting) important? What is the influence of the grain density as well as the fluid viscosity? Is the true distinction between both

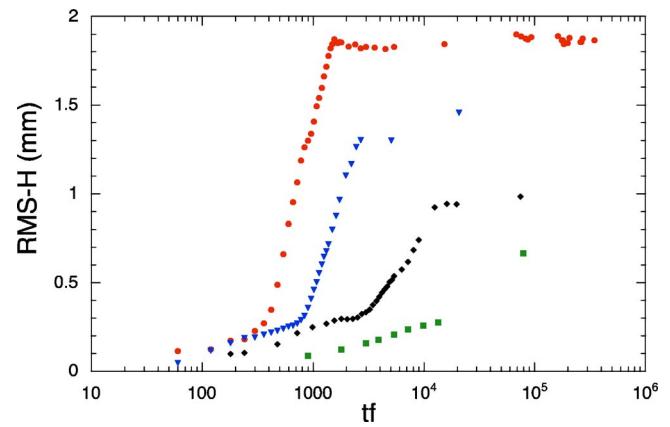


FIG. 12. (Color online) Root mean square value of the ripple height for several amplitudes (0.91, 1.22, 1.84, and 2.45 cm) as a function of time for cohesive grains (linear-log scale). Old setup. Parameters are $f=1$ Hz, $d=65$ μm .

types of ripples of hydrodynamical or granular origin? Our present experimental setup should allow in the near future a dynamical study of sand ripples and especially of the close coupling between the fluid flow and the grain motion.

ACKNOWLEDGMENTS

I am grateful to J. E. Wesfreid and A. Stegner for enlightening discussions. I am thankful to Denis Vallet, Olivier Brocard, and Christian Baradel for technical help. This work was supported by the A.C.I. "Jeunes Chercheurs" Grant No. 2314.

-
- [1] R. A. Bagnold, Proc. R. Soc. London, Ser. A **187**, 1 (1946).
 - [2] A. Stegner and J. E. Wesfreid, Phys. Rev. E **60**, R3487 (1999).
 - [3] G. Rousseaux, A. Stegner, and J. E. Wesfreid, Phys. Rev. E **69**, 031307 (2004).
 - [4] G. Rousseaux, H. Yoshikawa, A. Stegner, and J.-E. Wesfreid, Phys. Fluids **16**, 1049 (2004).
 - [5] K. H. Andersen, Phys. Fluids **13**, 58 (2001).
 - [6] U. Thiele, L. Bruschi, M. Bestehorn, and M. Bar, Eur. Phys. J. E **11**, 255 (2003).
 - [7] G. Rousseaux, H. Caps, and J.-E. Wesfreid, Eur. Phys. J. E **13**, 213 (2004).
 - [8] G. Rousseaux, Ph.D. thesis, Paris 6 University, 2003 (unpublished) (in French), <http://tel.ccsd.cnrs.fr/documents/archives/00/00/65/63/index-fr.html>
 - [9] P. Manneville, *Structures Dissipatives, Chaos et Turbulence* (Aléa, Saclay, 1991).
 - [10] T. Sekiguchi and T. Sunamura, Coastal Eng. **50**, 231 (2004).
 - [11] C. Faraci and E. Foti, Phys. Fluids **13**, 1624 (2001).
 - [12] J. Lundbeck Hansen *et al.*, Nature (London) **410**, 324 (2001).
 - [13] J. P. Davis, D. J. Walker, M. Townsend, and I. R. Young, J. Geophys. Res. **19**, C07020 (2004).
 - [14] B. T. Grasmeijer and M. G. Kleinans, Coastal Eng. **51**, 351 (2004).
 - [15] D. Smith and J. F. A. Sleath, Cont. Shelf Res. **25**, 485 (2005).
 - [16] M. A. Scherer, F. Melo, and M. Marder, Phys. Fluids **11**, 58 (1999).
 - [17] J. F. A. Sleath, *Sea Bed Mechanics* (Wiley, New York, 1984).
 - [18] P. Blondeaux, J. Fluid Mech. **218**, 1 (1990).
 - [19] K. W. Chan, M. H. I. Baird, and G. F. Round, Proc. R. Soc. London, Ser. A **330**, 537 (1972).
 - [20] P. Stevenson and R. B. Thorpe, Chem. Eng. Sci. **59**, 1295 (2004).